Rotors Drift Toward and Stabilize in Low Power Regions in Heterogeneous Models of Atrial Fibrillation

Laura Martinez-Mateu[1], Javier Saiz[2], Omer Berenfeld[3]

[1]Universidad Rey Juan Carlos, Móstoles, Spain
[2]Universitat Politècnica de València, Valencia, Spain
[3]University of Michigan, Ann Arbor, Michigan (USA)

Abstract

Atrial fibrillation (AF) afflicts more than 33 million people worldwide. Success of therapy strategies remains poor and better understanding of the arrhythmia and how to device more effective therapies are needed.

The aim of this work is to study the role of electric power distributions in rotors and AF dynamics. For this purpose, single cell and tissue simulations were performed to study the effect of ionic currents gradients and fibrosis in rotor's drifting. The root mean square of the ionic (P_{ion}), capacitance (P_c) and electrotonic (P_{ele}) power was computed over action potentials. Single cell simulations were performed for different values of I_{K1} and I_{CaL} and number of coupled myofibroblasts. Tissue simulations were performed in presence of I_{K1} and I_{CaL} gradients and diffused fibrosis.

Single cell simulations showed that P_{ion} and P_c increased with I_{K1}, while decreased by increasing I_{CaL}. Increasing the number of coupled myofibroblasts reduced P_{ion} and P_c, whereas P_{ele} increased. Finally, in tissue simulations rotors drifted to regions with low power and anchored in regions with higher density of blunted ionic induced power gradients.

1. Introduction

Atrial fibrillation (AF) is the most common sustained clinical arrhythmia affecting more than 33 million people worldwide, increasing morbidity and mortality, and is the leading cause of embolic stroke [1], [2]. For patients with AF, antiarrhythmic drugs perform poorly and ablation has been demonstrated to be superior to pharmacologic therapy in maintaining sinus rhythm (SR). Despite its controversial success rate and long-term effects, ablation is often the only therapy available [3], [4].

AF is a heterogeneous progressive arrhythmia and regardless of its stage, possible alterations of the atrial substrate electrophysiological parameters might provoke triggered activity or conduction blocks leading to reentry and arrhythmia [5]. However, the understanding of fibrillation in humans is still limited due to our poor knowledge of how rotors spontaneously initiate, drift, stabilize, or terminate under conditions of multi-factorial substrate heterogeneity and remodelling. The energy and its temporal rate (power) domain parametrization of the cardiac electrical activity carries the integral characterization of the voltages and currents during the cellular and coupling excitation process. As such, power analysis can capture dynamical and fixed features of the substrate and its excitation which are missed in analyses of voltage signals as have been performed in either the time, frequency or the phase domains.

In this proof-of-concept work we aim to study the role of electric power values and gradients induced by altering I_{K1}, I_{CaL} and fibrosis in rotors dynamics and drifts. We hypothesize that energy domain parametrization would predict localization of stable reentries capable of leading to AF sustenance.

2. Methods

We conducted computer simulations on single cells and two-dimensional (2D) tissue models of atrial activity.

2.1. Single cell computer simulations

The Koivumäki et al. models [6], [7] were used to reproduce the electrical activity of atrial myocytes and myofibroblasts under SR conditions. Models were stabilized for 1 minute at a basic cycle length (BCL) of 1 s. To study the influence of ionic currents and fibrosis on single cell power, I_{K1} and I_{CaL} were varied from 0.75 up to 2 their basal value and 1 to 5 myofibroblasts were coupled to a single atrial myocyte. Then, for each single cell simulations, ionic (P_{ion}), capacitance (P_c) and electrotonic (P_{ele}) power terms were calculated (see

section 2.3 below). The root mean square (RMS) value of the instantaneous power was calculated for the last 3 beats in each simulation between the depolarization time and the 90% action potential repolarization time.

2.2. Tissue computer simulations

2D computer simulations on a 4.98 cm × 4.98 cm sheet comprising of 27,889 nodes 0.03 cm apart and 27,556 quadrangular elements, were performed. Rotors were induced by applying a cross-field stimulation protocol S1-S2, as shown in Figure 1 (a).

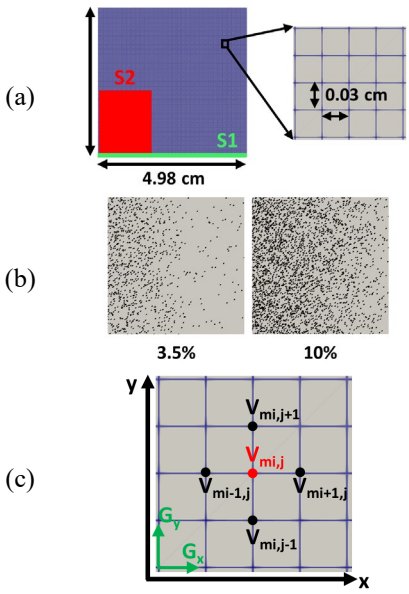

Figure 1. Geometrical mesh showing the stimulation protocol (a), diffused fibrosis patterns (b) and nomenclature of V_m (same for I_{ion}, C_m and G) throughout the nodes for computing the power at node i,j (c).

Electrical propagation of action potentials was simulated by solving the mono-domain reaction-diffusion formulation

$$\nabla \cdot (D\nabla V_m) = C_m \frac{\partial V_m}{\partial t} + I_{ion} \quad (1)$$

using the finite elements method [8] at 0.01 ms time step. In Equation (1) D is the conductivity tensor, V_m the membrane potential, C_m the membrane capacitance and I_{ion} is the sum of all the trans-membrane ionic currents.

The Koivumäki et al. model was used to reproduce the electrical activity of atrial myocytes in persistent AF conditions [9] and of atrial myofibroblasts [7]. The maximum conductance of I_{Kr} and coupling in the model were modified [10] to emulate the electrophysiological heterogeneity and anisotropy ratio observed in the left atrium (LA) [11] with fibers oriented in the vertical axis. I_{K1} and I_{CaL} were varied about 15% from their basal value to produce horizontal ionic currents gradients (between the left to right edge of the 2D tissue and vice versa). Two random diffused fibrosis patterns with 3.5% and 10% myofibroblasts density were incorporated over the whole tissue. As shown if Figure 1 (b), myofibroblasts local density gradually decreased from the left to right boundary of the tissue model. Different combinations of ionic gradients and fibrosis were tested. Finally, rotors' trajectories were tracked by phase singularities detection in phase movies [10]. The RMS of the P_{ion}, P_c and P_{ele}, as well as the total power (P_{Tot}) were calculated for the duration of the phase singularity tracking.

2.3. Power analysis

To carry out the power analysis of the simulations, a temporal resolution of 0.1 ms was used. In addition, for tissue simulations a down-sampled spatial resolution of 0.09 cm was employed. P_{ion}, P_c, P_{ele} and P_{Tot} were calculated at each node i,j as follows (see Figure 1 (c)):

$$P_{ion_{i,j}} = V_{m_{i,j}} I_{ion_{i,j}} \quad (2)$$

$$P_{c_{i,j}} = C_{m_{i,j}} \frac{\partial V_{m_{i,j}}}{\partial t} \quad (3)$$

$$P_{ele_{i,j}} = \frac{1}{2}\Big(G_{x_{i-1,j}}\left(V_{m_{i,j}} - V_{m_{i-1,j}}\right)^2 + G_{x_{i,j}}\left(V_{m_{i+1,j}} - V_{m_{i,j}}\right)^2 + G_{y_{i,j-1}}\left(V_{m_{i,j}} - V_{m_{i,j-1}}\right)^2 + G_{y_{i,j}}\left(V_{m_{i,j+1}} - V_{m_{i,j}}\right)^2\Big) \quad (4)$$

$$P_{Tot} = P_{ion} + P_c + P_{ele} \quad (5)$$

3. Results

Power graphs in Figure 2 (a) and (b) for single cell simulations show that P_{ion} and P_c at baseline were about 40 pW and 1.25 pW, respectively. Both powers increased with I_{K1} to 64 pW (P_{ion}) and 1.6 pW (P_c) when I_{K1} doubled (Figure 2(a)), while decreased by increasing I_{CaL} to 38 pW (P_{ion}) and 1.19 pW (P_c) when I_{CaL} doubled (Figure 2(b)). Increasing the number of myofibroblasts coupled to the single myocyte reduced P_{ion} and P_c to 8 pW and 0.6 pW for 5 coupled myofibroblasts, respectively, whereas P_{ele} increased from 0 pW to 6 pW (Figure 2(c)).

Results corresponding to 2D tissue simulations are summarized in Figure 3. As illustrated, rotors drifted to regions with lower I_{K1} values (low P_{Tot}) and initiated or drifted to regions with higher I_{CaL} values (low P_{Tot}), thus offering an opposite effect on rotors drifting (see Figure 3 (a-d)). When combining I_{K1} and I_{CaL} gradients, rotors drifted to the region of tissue with lower I_{K1} and I_{CaL} values, showing the dominance of the I_{K1} over I_{CaL} gradient (see Figure 3 (e-f)). The area of high local density of diffused fibrosis anchored the rotor (Figure 3 (g)). With the presence of similar fibrosis distribution,

rotors anchored in the region with higher I_{K1} (Figure 3 (h)), indicating an attraction of rotors toward more dense diffused fibrosis areas predominated ionic gradient here.

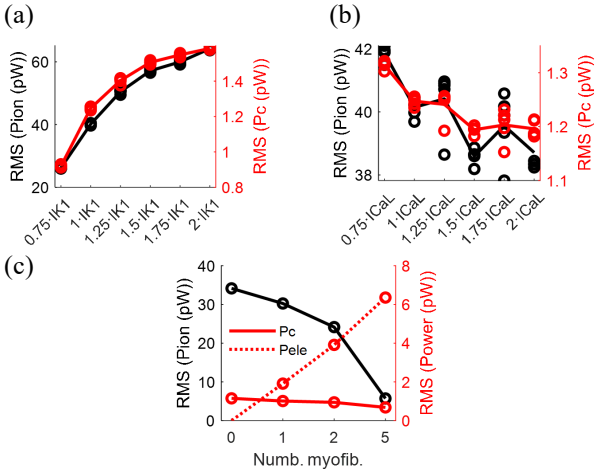

Figure 2. RMS power for single cell simulations when varying I_{K1} (a), I_{CaL} (b) and the number of coupled myofibroblasts to a single myocyte (c). P_{ion} in black and P_c and P_{ele} in red. Circles correspond to the power value of the last three beats of the simulation.

In general, the drift trajectories of rotors on the RMS power maps show stabilization at the minimal P_{Tot} and P_{ele} approximated vertical bands (blue regions with a sigmoid shape in Figure 3 (2) and (5)), which are quite narrow and elongated. It should be noted that the distribution of P_{Tot} (Figure 3 (2)) is very similar to the distribution of P_{ele} (Figure 3 (5)) which suggest that P_{ele} is the largest contribution to P_{Tot} (P_{ele} has μW magnitude compared to pW for P_{ion} and P_c). However, although P_{ion} and P_c levels are smaller, they seem to be associated also with the rotors drifting that stabilize at the center of maximal P_{ion} and minimal P_c circular red and blue regions, respectively, depicted in Figure 3 (3-4).

In preliminary simulations with 10% fibrosis reentries were not induced, or they did not last for the whole simulation time. As an example, results of simulation with I_{K1} gradient and 10% fibrosis are depicted in Figure 4. In this case, rotor lasted less than 2 s. The rotor was initiated in a medium-high density fibrosis region and high values of I_{K1}, similar to the initiation site in the simulation with 3.5% fibrosis, and thereafter the rotor drifted toward the left side of the tissue, where the amount of myofibroblasts and the I_{K1} values were even higher, until extinction at the border where P_{Tot}, P_{ele} and P_c were minimal and P_{ion} was maximal.

4. Discussion

The aim of this work was to provide an initial elucidation on the role of ionic currents gradients and fibrosis and their power characterization in rotor's drifting. For this purpose, single cell and 2D tissue simulations were performed. Our results showed that rotors drifted towards low I_{K1} values, high I_{CaL} values and more dense fibrosis regions, and stabilize in low power regions on P_{Tot} maps. Among the model configurations tested here, there was a dominance of fibrosis over I_{K1} gradient, and in turn of I_{K1} gradient over I_{CaL} gradient. Our results are in accordance with literature. In previous works it was demonstrated that rotors were attracted from LA to pulmonary veins, where I_{K1} and I_{CaL} were smaller [12] and that rotors anchored in the border of fibrotic regions [13], [14]. In this study, the combination of I_{K1} and I_{CaL} gradients also yielded a rotor drifting towards the region with lower I_{K1} and I_{CaL} and presence of fibrosis attracted rotors. In our case, rotors probably drifted inside the fibrotic region due to the diffused character of the fibrosis tested, unlike in the cited studies where rotors were anchored to the border of patchy fibrosis, probably due to a complete propagation blockade at high density of fibroblasts inside the patch.

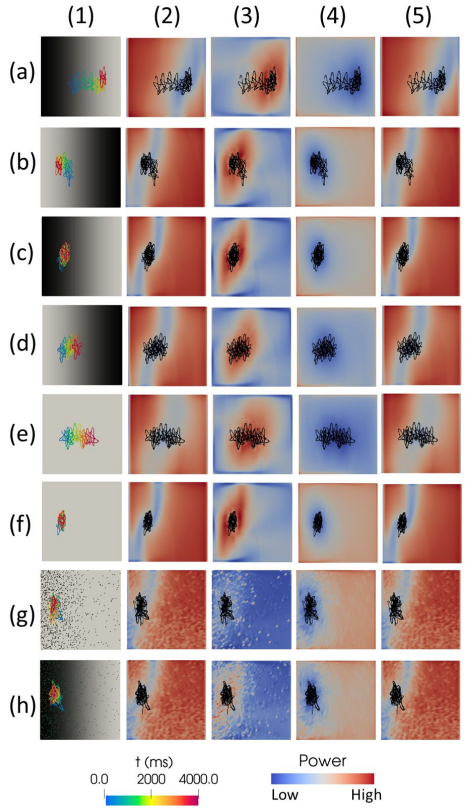

Figure 3. Rotors' trajectories and RMS power maps corresponding to tissue simulations. (a,b) I_{K1} gradients; (c,d) I_{CaL} gradients; (e) simultaneous I_{K1} as in (a) and I_{CaL} as in (c) gradients; (f) simultaneous I_{K1} as in (b) and I_{CaL} as in (d) gradients; (g) 3.5% fibrosis; and (h) 3.5% fibrosis with I_{K1} gradient as in (a). (1) Rotors' trajectories. Low to high values of ionic gradients are depicted from grey to black; (2) P_{Tot}; (3) P_{ion}; (4) P_c; (5) P_{ele}.

Finally, when comparing the power levels in single cell and 2D tissue results, we observed that P_{ion} and P_c increased by increasing I_{K1} and decreasing I_{CaL} and the amount of couped myofibroblasts, and P_{ele} increased with the number of coupled myofibroblasts. These distinct dependencies are not clearly observed on the 2D power maps, probably because the simulated activation rate of coupled myocytes in the tissue differs from the isolated myocytes in single cell simulations. Further numerical and experimental research is required to elucidate on the relationship between the power of the various action potential factors and the rotors drift and stabilization.

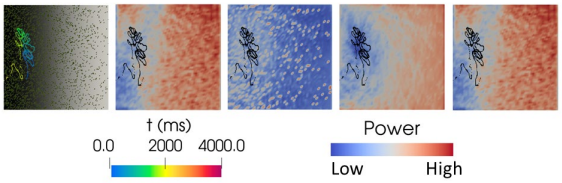

Figure 4. Rotors' trajectories and RMS power maps corresponding to a simulation with 10% diffused fibrosis and I_{K1} gradient. From left to right: rotor' trajectory (low to high values of I_{K1} gradient depicted from grey to black), P_{Tot}, P_{ion}, P_c and P_{ele}.

5. Conclusions

Our simulation results suggest that gradients in ionic currents and diffused fibrosis affect drifts of rotors whereby fibrosis is a dominating factor, followed by I_{K1} and I_{CaL}. In addition, the effects of the powers (P_{ion}, P_c, P_{ele}) on drift may not necessarily be proportional to their levels. Rotors stabilize in low power regions when considering all power contributions (P_{Tot}). However, detection of regions with maximal P_{ion} and minimal P_c might also help to identify areas where rotors stabilize.

Acknowledgments

Supported in part by grants from the National Institutes of Health R01-HL118304, R21-HL153694, R21-EB032661 (Berenfeld) and R01-HL156961 (Berenfeld, Saiz), and the Ministerio de Economía y Competitividad PID2019-104356RB-C42 and PID2019-104356RB-C41.

References

[1] E. J. Benjamin *et al.*, "American Heart Association Statistics C and Stroke Statistics S. Heart Disease and Stroke Statistics-2017 Update: A Report From the American Heart Association.," *Circulation*, vol. 135, pp. e146–e603, 2017.

[2] G. A. Roth *et al.*, "Global, Regional, and National Burden of Cardiovascular Diseases for 10 Causes, 1990 to 2015.," *J. Am. Coll. Cardiol.*, vol. 70, pp. 1–25, 2017.

[3] P. Kirchhof *et al.*, "2016 ESC Guidelines for the management of atrial fibrillation developed in collaboration with EACTS," *Eur. Heart J.*, vol. 37, no. 38, pp. 2893–2962, 2016.

[4] A. Hakalahti, F. Biancari, J. C. Nielsen, and M. J. P. Raatikainen, "Radiofrequency ablation vs. antiarrhythmic drug therapy as first line treatment of symptomatic atrial fibrillation: systematic review and metaanalysis.," *Europace*, vol. 17, pp. 370–378, 2015.

[5] J. Heijman, J. B. Guichard, D. Dobrev, and S. Nattel, "Translational Challenges in Atrial Fibrillation.," *Circ. Res.*, vol. 122, pp. 752–773, 2018.

[6] J. T. Koivumaki, T. Korhonen, and P. Tavi, "Impact of sarcoplasmic reticulum calcium release on calcium dynamics and action potential morphology in human atrial myocytes: a computational study," *PLoS Comput Biol*, vol. 7, no. 1, p. e1001067, 2011.

[7] J. Koivumäki *et al.*, "Na+ current expression in human atrial myofibroblasts: Identity and functional roles," *Front. Physiol.*, vol. 5 JUL, no. August, pp. 1–14, 2014.

[8] E. A. Heidenreich, J. M. Ferrero, and J. . Doblare M. Rodríguez, "Adaptive Macro Finite Elements for the Numerical Solution of Monodomain Equations in Cardiac Electrophysiology," *Ann. Biomed. Eng.*, vol. 38, no. 7, pp. 2331–2345, Jul. 2010.

[9] J. T. Koivumäki, G. Seemann, M. M. Maleckar, and P. Tavi, "In Silico Screening of the Key Cellular Remodeling Targets in Chronic Atrial Fibrillation," *PLoS Comput. Biol.*, vol. 10, no. 5, 2014.

[10] L. Martinez-Mateu *et al.*, "Factors affecting basket catheter detection of real and phantom rotors in the atria: A computational study," *PLoS Comput. Biol.*, vol. 14, no. 3, pp. 1–26, 2018.

[11] D. Li, L. Zhang, J. Kneller, and S. Nattel, "Potential ionic mechanism for repolarization differences between canine right and left atrium.," *Circ. Res.*, vol. 88, pp. 1168–1175, 2001.

[12] C. J. Calvo, M. Deo, S. Zlochiver, J. Millet, and O. Berenfeld, "Attraction of rotors to the pulmonary veins in paroxysmal atrial fibrillation: A modeling study," *Biophys. J.*, vol. 106, no. 8, pp. 1811–1821, 2014.

[13] R. Morgan, M. A. Colman, H. Chubb, G. Seemann, and O. V. Aslanidi, "Slow conduction in the border zones of patchy fibrosis stabilizes the drivers for atrial fibrillation: Insights from multi-scale human atrial modeling," *Front. Physiol.*, vol. 7, no. OCT, pp. 1–15, 2016.

[14] S. Zahid *et al.*, "Patient-derived models link re-entrant driver localization in atrial fibrillation to fibrosis spatial pattern," *Cardiovasc. Res.*, vol. 110, no. 3, pp. 443–454, 2016.

Address for correspondence:

Laura Martinez-Mateu.
Universidad Rey Juan Carlos, Departamental III, Camino del Molino Nº5, 28942, Fuenlabrada, Madrid
laura.martinez.mateu@urjc.es